

# Concentration-Dependent Cellular Uptake of Graphene Oxide Quantum Dots Promotes the Odontoblastic Differentiation of Dental Pulp Cells via the AMPK/mTOR Pathway

Ling Lin, Yexin Zheng, Chao Wang, Pei Li, Duoling Xu,\* and Wei Zhao\*



Cite This: *ACS Omega* 2023, 8, 5393–5405



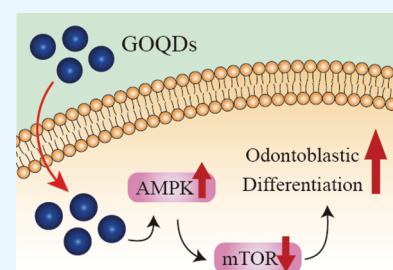
Read Online

ACCESS |

Metrics & More

Article Recommendations

**ABSTRACT:** As zero-dimension nanoparticles, graphene oxide quantum dots (GOQDs) have broad potential for regulating cell proliferation and differentiation. However, such regulation of dental pulp cells (DPSCs) with different concentrations of GOQDs is insufficiently investigated, especially on the molecular mechanism. The purpose of this study was to explore the effect and molecular mechanism of GOQDs on the odontoblastic differentiation of DPSCs and to provide a theoretical basis for the repair of pulp vitality by pulp capping. CCK-8, immunofluorescence staining, alkaline phosphatase activity assay and staining, alizarin red staining, qRT-PCR, and western blotting were used to detect the proliferation and odontoblastic differentiation of DPSC coculturing with different concentrations of GOQDs. The results indicate that the cellular uptake of low concentration of GOQDs (0.1, 1, and 10  $\mu\text{g}/\text{mL}$ ) could promote the proliferation and odontoblastic differentiation of DPSCs. Compared with other concentration groups, 1  $\mu\text{g}/\text{mL}$  GOQDs show better ability in such promotion. In addition, with the activation of the AMPK signaling pathway, the mTOR signaling pathway was inhibited in DPSCs after coculturing with GOQDs, which indicates that low concentrations of GOQDs could regulate the odontoblastic differentiation of DPSCs by the AMPK/mTOR signaling pathway.



## 1. INTRODUCTION

Caries and crown fracture are common dental hard tissue disease, which can cause the exposure or close proximity of pulp tissue and ultimately result in inflammation of pulp and periapical tissue.<sup>1</sup> Pulp capping is a conservative treatment for extensively dental defect.<sup>2</sup> This treatment can induce reparative dentinogenesis by applying biomaterial to the dentine close to the pulp or to the exposed pulp tissue and then protecting the pulp from noxious stimuli.<sup>3</sup> As shown in Figure 1, localized dental defect may lead to destruction of primary odontoblast. However, the application of a pulp capping agent can induce the dental pulp cells (DPSCs) to differentiate into odontoblast-like cells, which can form reparative dentin to protect the pulp tissue.<sup>4</sup> Therefore, a better material to promote odontoblastic differentiation is of vital significance for the success of pulp capping.

As stem cells, the cell fate of DPSCs is determined by a series of complex transcription factors and epigenetic networks.<sup>5</sup> The physiological niche that controls cell fate is composed of a cell microenvironment, which can affect cell behaviors, including self-renewal and differentiation. In biomedical applications, nanomaterials can serve as the physiological niche for the formation and differentiation of stem cells. The physical and chemical properties of nanomaterials can affect the cell microenvironment and then regulate the cellular response to differentiation.<sup>6</sup> Nanomaterials refer to particles with a size range of 1–100nm,<sup>7</sup> with the advantages of

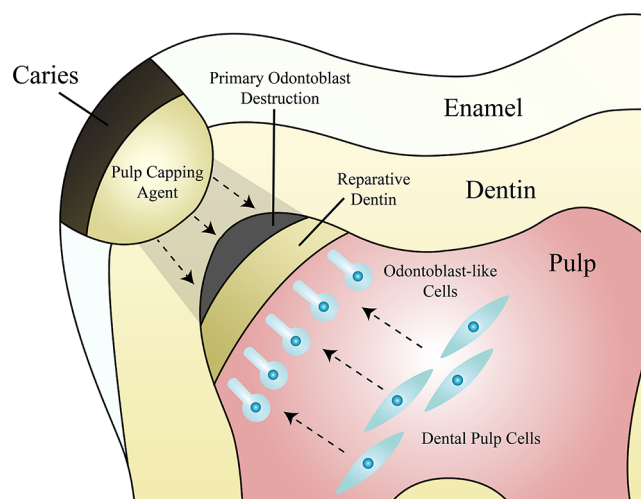


**Figure 1.** Effect of pulp capping agent. Pulp capping agent can induce DPSCs to differentiate into odontoblast-like cells, which can form reparative dentin to protect the pulp tissue.

Received: October 10, 2022

Accepted: January 16, 2023

Published: February 1, 2023



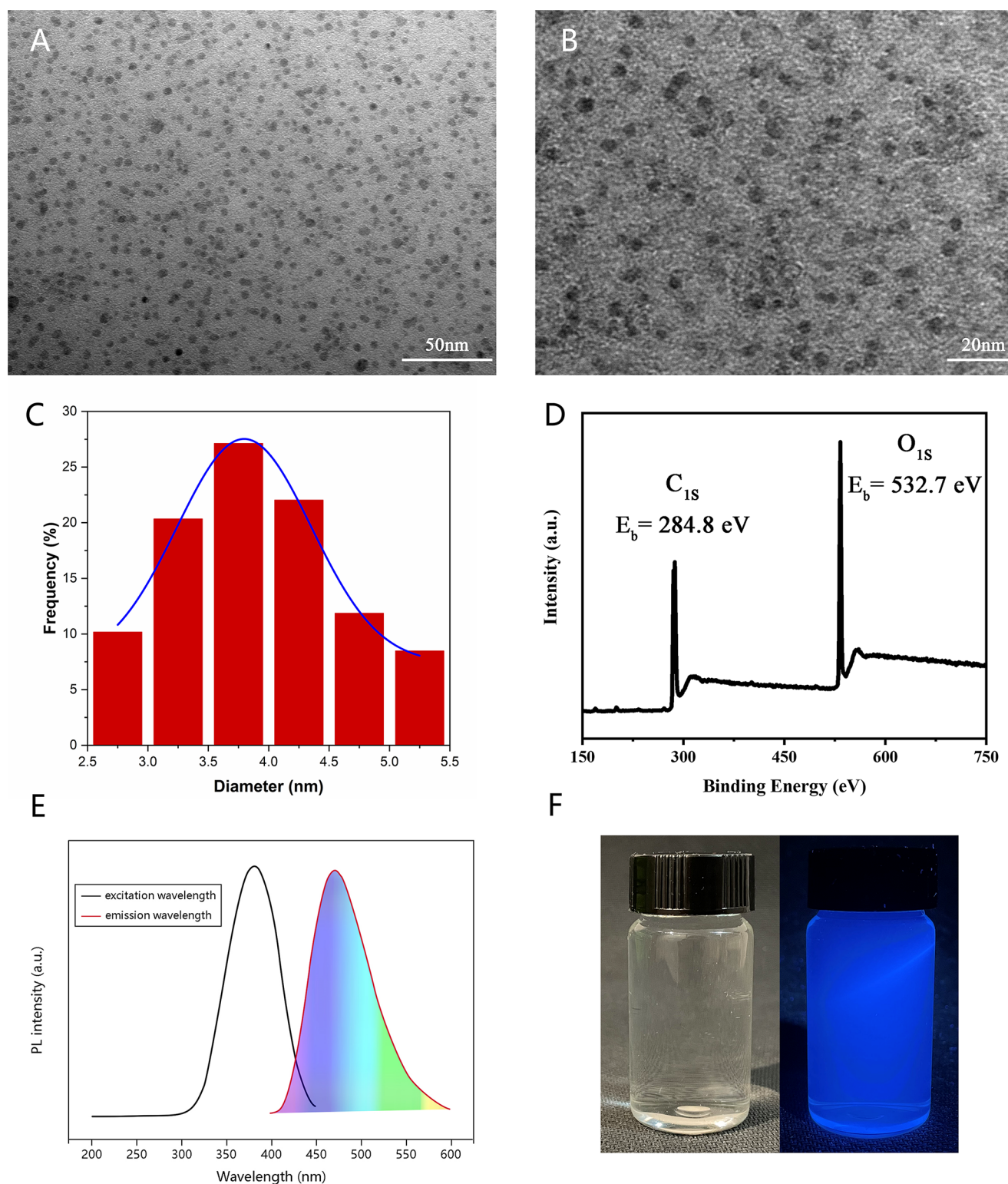


**Figure 2.** Characterization of GOQDs. (A, B) TEM image of GOQDs; (C) size distribution of GOQDs; (D) XPS survey peaks of GOQDs; (E) excitation wavelength and emission wavelength of GOQDs; (F) photos of GOQDs colloid under natural light (left) and at 365 nm UV lamp (right).

penetrating across cell barriers and preferential accumulation in specific cells, which provide therapeutic and diagnostic properties.<sup>8</sup>

According to different dimensional structures, nanostructures can be divided into zero dimensional (quantum dots), one dimensional (nanotubes, nanofibers, and nanowires), two

dimensional (nanosheets, nanodiscs, and nanowalls) and three dimensional (hollow spheres and nanoflowers).<sup>9</sup> Quantum dots are nanoscale (2–10 nm) fluorescent particles composed of semiconductor materials.<sup>10</sup> Except from the excellent properties of graphene oxide (GO) itself, as zero dimensional nanoparticles, graphene oxide quantum dots (GOQDs) also

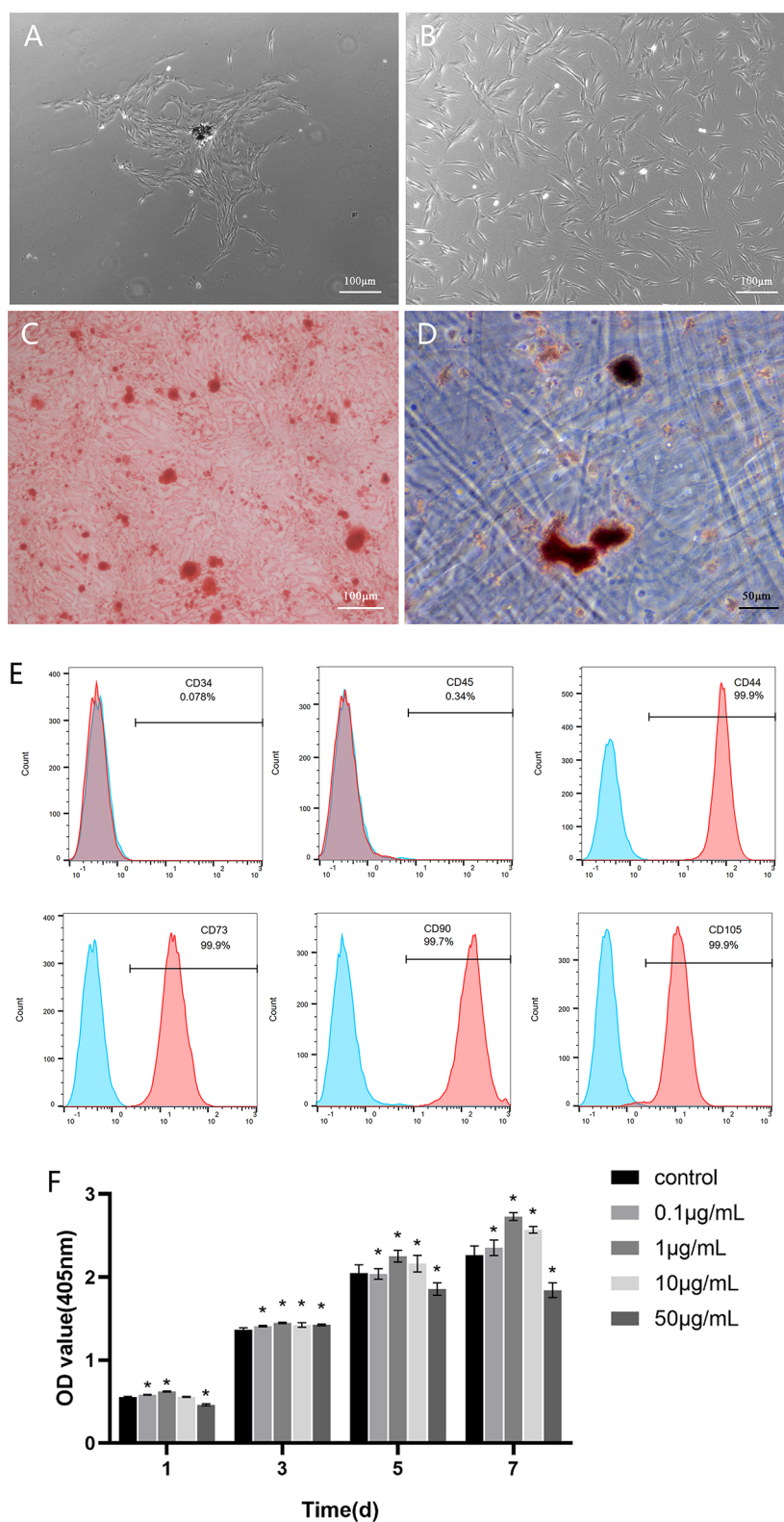


**Figure 3.** Characterization and proliferation of DPSCs. (A) 3 days of primary DPSCs,  $\times 50$ ; (B) DPSCs at P3,  $\times 50$ ; (C) cells were treated with osteogenic induction medium after 14 days and stained with Alizarin red,  $\times 50$ ; (D) cells were treated with adipogenic induction medium after 21 days and stained with oil red,  $\times 100$ ; (E) flow cytometry analysis of cell surface marker CD34, CD45, CD44, CD73, CD90, CD105; (F) proliferation of DPSCs cocultured with different concentrations (0, 0.1, 1, 10, and 50  $\mu\text{g/mL}$ ) of GOQDs for 1, 3, 5, and 7 days ( $*p < 0.05$  vs the control group).

have a higher surface area to volume ratio and smaller size.<sup>5</sup> Therefore, compared with other dimensional nanostructures, quantum dots have more active sites and unique physical and

chemical properties.<sup>9</sup> Studies have shown that a higher surface area to volume ratio could lead to more proteins adsorbed on the surface of quantum dots, which will change the properties

of the surface and size of the nanoparticle and then promote cellular internalization through the internalization pathway mediated by clathrin.<sup>8</sup> The size and morphology of nanoparticles can influence their penetration into cells. Compared with nanorods of the same size, nanospheres are easier to enter cells.<sup>11</sup> The nanoscale size and well dispersibility provide graphene quantum dots (GQDs) and their derivatives with good cell permeability.<sup>12</sup> In addition, GQD-like materials can exert an antibacterial effect by inducing the generation of reactive oxygen species,<sup>13</sup> and this antibacterial effect can be significantly enhanced under photoexcitation.<sup>14</sup> Studies found that the materials loaded with GOQDs can significantly enhance the antibacterial activity against *Escherichia coli* and *Staphylococcus aureus*<sup>15</sup> and improve the wound healing effect.<sup>16</sup>

The perturbation caused by nanoparticle to normal homeostasis of cells could affect their function and behavior, and the cellular internalization of quantum dots has important influence on the differentiation of stem cells.<sup>17</sup> Both the mechanical stress in cells induced by quantum dots and the surface modification of quantum dots play an important role in determining the differentiation of mesenchymal stem cells (MSCs).<sup>5</sup> In addition, many studies have also shown that the regulation of differentiation caused by GQDs and their derivatives depended on the interaction between quantum dots and specific cellular signal pathways. For example, GQDs and their derivatives have been proved to have the ability to promote osteogenic differentiation of MSCs by up regulating bone morphogenetic protein (BMP), TGF- $\beta$ , and Wnt signaling pathways.<sup>17</sup> Our previous studies confirmed that GOQDs at a specific concentration can promote the osteogenic differentiation of stem cells from human exfoliated deciduous teeth<sup>18</sup> and bone marrow mesenchymal stem cells<sup>19</sup> by Wnt signaling pathways.

As a common classification of autophagy regulators, many nanomaterials have the potential in balancing autophagy homeostasis,<sup>20</sup> especially quantum dots.<sup>21</sup> Quantum dots can induce oxidative stress and autophagy, thus regulating cell behavior through mTOR, MAPK, and other signal pathways.<sup>22</sup> By the cellular protection mechanism, quantum dots with smaller sizes are more effective in autophagy induction.<sup>8</sup> Study has confirmed that GOQDs can induce autophagy through various ways.<sup>23</sup> As a coordinated intracellular process, autophagy can remove unnecessary or dysfunctional cellular components by degradation and recycling<sup>24</sup> and then maintain cell homeostasis.<sup>25</sup> Therefore, autophagy is considered to be a significant process for stem cells to maintain stemness, including the proliferation, self-renewal, and directional differentiation.<sup>26</sup> This process plays an important role in odontoblastic differentiation of DPSCs during tooth bud development and reparative dentinogenesis.<sup>27</sup> In addition, a study has shown that autophagy can promote the differentiation of odontoblast for the resistance to bacterial invasion and stimulate subodontoblast layer cell differentiation into an odontoblast-like cell for the production of reactionary dentin.<sup>28</sup>

The initiation of autophagy is regulated by two critical components of the nutrient/energy sensor pathway: mammalian target of rapamycin (mTOR) and AMP-activated protein kinase (AMPK).<sup>29</sup> Studies have shown that graphene-based nanomaterials may signal through TLR receptors to induce ROS stress and then trigger an autophagic response in cells by AMPK/mTOR or MAPK signaling pathways.<sup>30</sup> Although a variety of signaling cascades and regulatory mechanisms can

influence autophagy, AMPK may be the most conserved autophagy inducer in biological evolution for its relationship with autophagy degradation in almost all eukaryotic cells.<sup>31</sup> AMPK is an evolutionarily conserved serine/ threonine protein kinase. As an energy sensor, AMPK can regulate cell metabolism to maintain energy homeostasis.<sup>32</sup> In contrary, autophagy is inhibited by mTOR. mTOR belongs to the phosphatidylinositol-3 kinases (PI3K)-related kinase (PIKK) family, which can sense and integrate various environmental and intracellular signals to regulate cellular and organismic responses.<sup>33</sup> Activated AMPK can inhibit mTOR and ultimately lead to autophagy.<sup>34</sup> The functions of AMPK and mTOR, which correlate with autophagy signaling, have been confirmed in the osteogenic differentiation of mesenchymal stem cells.<sup>25,35</sup>

In this study, we speculated that the cellular uptake of GOQDs in a proper concentration range can promote the odontoblastic differentiation of DPSC through the AMPK/mTOR signaling pathway due to the characteristics of quantum dots. Furthermore, we will explore the appropriate concentration range of GOQDs for promoting odontoblastic differentiation, which will indicate whether this effect is concentration-dependent.

## 2. RESULTS

**2.1. Characterization of GOQDs.** The morphology of GOQDs was observed by transmission electron microscopy (TEM, Hitachi, Japan). GOQDs are dispersed with the diameters of 2.5–5.5 nm (Figure 2A–C). The chemical composition of the material can be determined by X-ray photoelectron spectroscopy (XPS). XPS shows two prominent peaks, C<sub>1s</sub> (284.8 eV) and O<sub>1s</sub> (532.7 eV) (Figure 2D), which prove that the GOQD sample contains only carbon and oxygen, with no other impurity elements mixed. Having many oxygen-containing functional groups is a characteristic that distinguishes the GOQDs from the GQDs.

**2.2. Characterization of DPSCs.** The major morphology of DPSCs was spindle-like or fibroblast-like (Figure 3B). After the osteogenic and adipogenic induction of DPSCs, the formation of calcium nodules and lipid droplet was observable (Figure 3C,D). In the analysis of cell-surface markers, 99.9% of the cells were CD44-positive, 99.9% were CD73-positive, 99.7% were CD90-positive, and 99.9% were CD105-positive; only 0.078% of cells were CD34-positive and 0.34% were CD45-positive (Figure 3E). These results show that the expression of mesenchymal stem cell related markers was positive, as the expression of hematopoietic markers was negative, which indicated that DPSCs were mesenchymal stem cell with multiple differentiation potential.

**2.3. Cell Proliferation and Cellular Uptake of GOQDs.** The proliferation ability of DPSCs cocultured with different concentrations of GOQDs was measured by CCK-8 assay. DPSCs were cocultured with a medium, which include different concentrations (0, 0.1, 1, 10, and 50  $\mu\text{g}/\text{mL}$ ) of GOQDs for 1, 3, 5, and 7 days. According to the result (Figure 3F), GOQDs showed low cytotoxicity at low concentration (0.1, 1, and 10  $\mu\text{g}/\text{mL}$ ). The proliferation of DPSCs was significantly promoted with 1 and 10  $\mu\text{g}/\text{mL}$  GOQDs. On the contrary, when the concentration of GOQDs reaches 50  $\mu\text{g}/\text{mL}$ , it shows an obvious inhibitory effect of the proliferation of DPSCs.

The location of GOQDs and the morphology of DPSCs cocultured with GOQDs were observed by confocal laser

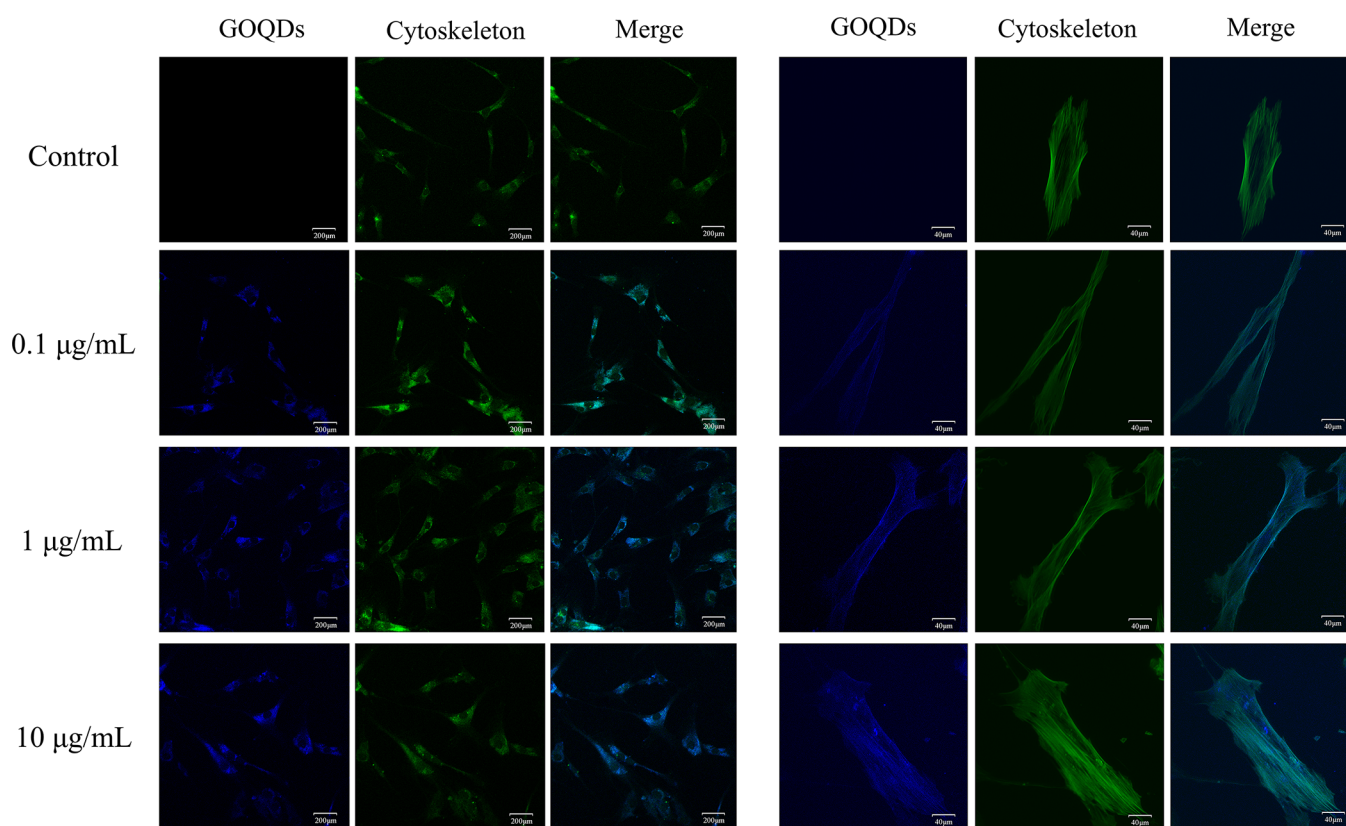


**Figure 4.** Confocal laser scanning microscopy images of DPSCs cocultured with different concentrations (0, 0.1, 1, and 10  $\mu\text{g/mL}$ ) of GOQDs for 72 h.

scanning microscopy. As shown in Figure 4, after coculturing with GOQDs for 72 h, DPSCs in each concentration group (0.1, 1, and 10  $\mu\text{g/mL}$ ) exhibited normal spindle-like morphology at high magnification compared with the control group. Furthermore, after coculturing with GOQDs for 72 h, DPSCs emitted blue fluorescence under 405 nm of excitation wavelength, which cannot be observed in the control group. This phenomenon indicated that there was cellular uptake of GOQDs happening in DPSCs: GOQDs can penetrate the cell membrane and locate in the cytoplasm, by which these nanoparticles can exert a certain effect.

**2.4. ALP Activity Assay and ALP Staining.** DPSCs were cocultured with odontogenic induction medium (OIM), which include different concentrations (0.1, 1, and 10  $\mu\text{g/mL}$ ) of GOQDs for 7 and 14 days, and then the activity of ALP was detected by the ALP assay and ALP staining. The result of the ALP assay (Figure 5B,C) suggests that after 7 days of coculture, DPSCs treated with 1  $\mu\text{g/mL}$  GOQDs show higher ALP activity compared with the control group, and there was no statistical difference between the other concentration groups and the control group. This indicated that 1  $\mu\text{g/mL}$  of GOQDs could play a promoting role in the early stage of odontoblast differentiation. After 7 and 14 days of coculture, DPSCs treated with GOQDs show higher ALP activity compared with the control group, of which DPSCs treated with 1  $\mu\text{g/mL}$  GOQDs had the highest activity of ALP. The ALP staining of DPSCs cocultured for 7 days has the same trend of result compared with the ALP assay (Figure 5A), which indicated that low concentration of GOQDs (0.1, 1, and 10  $\mu\text{g/mL}$ ) can promote mineralization of DPSCs.

**2.5. Alizarin Red Staining.** DPSCs were cocultured with OIM, which include different concentrations (0.1, 1, and 10  $\mu\text{g/mL}$ ) of GOQDs for 14 days, and then the deposition of calcium nodules was evaluate by Alizarin red staining. The result shows that DPSCs treated with 1 and 10  $\mu\text{g/mL}$  GOQDs have more obvious deposition of calcium nodules, which manifested in both the quantity and diameter of calcium nodules (Figure 5D). In the semi-quantitative interpretation of Alizarin red staining, the results of DPSCs treated with 1 and 10  $\mu\text{g/mL}$  GOQDs were 165 and 149% higher than the control group, respectively, while there were no significant differences between 0.1  $\mu\text{g/mL}$  GOQD group and the control group (Figure 5E).

**2.6. qRT-PCR and Western Blotting.** DPSCs were cocultured with OIM, which include different concentrations (0.1, 1, and 10  $\mu\text{g/mL}$ ) of GOQDs for 7 and 14 days, and then qRT-PCR and western blotting were used to detect the expression levels of odontoblastic differentiation related genes and proteins in DPSCs. The result of qRT-PCR (Figure 6A,B) shows that on the 7th and 14th days of odontogenic induction, compared with the control group, the expression levels of ALP and Runx2 increased in the 1  $\mu\text{g/mL}$  GOQD group and 10  $\mu\text{g/mL}$  GOQD group, and the expression of DSPP and DMP-1 increased significantly. Western blotting analysis (Figure 6C–F) shows that the expression levels of odontogenic proteins increased significantly in the 1  $\mu\text{g/mL}$  GOQD group and 10  $\mu\text{g/mL}$  GOQDs group after 14 days of odontogenic induction. These results suggest that GOQDs at the concentration of 1 or 10  $\mu\text{g/mL}$  can promote the odontoblastic differentiation of DPSCs, and the optimum

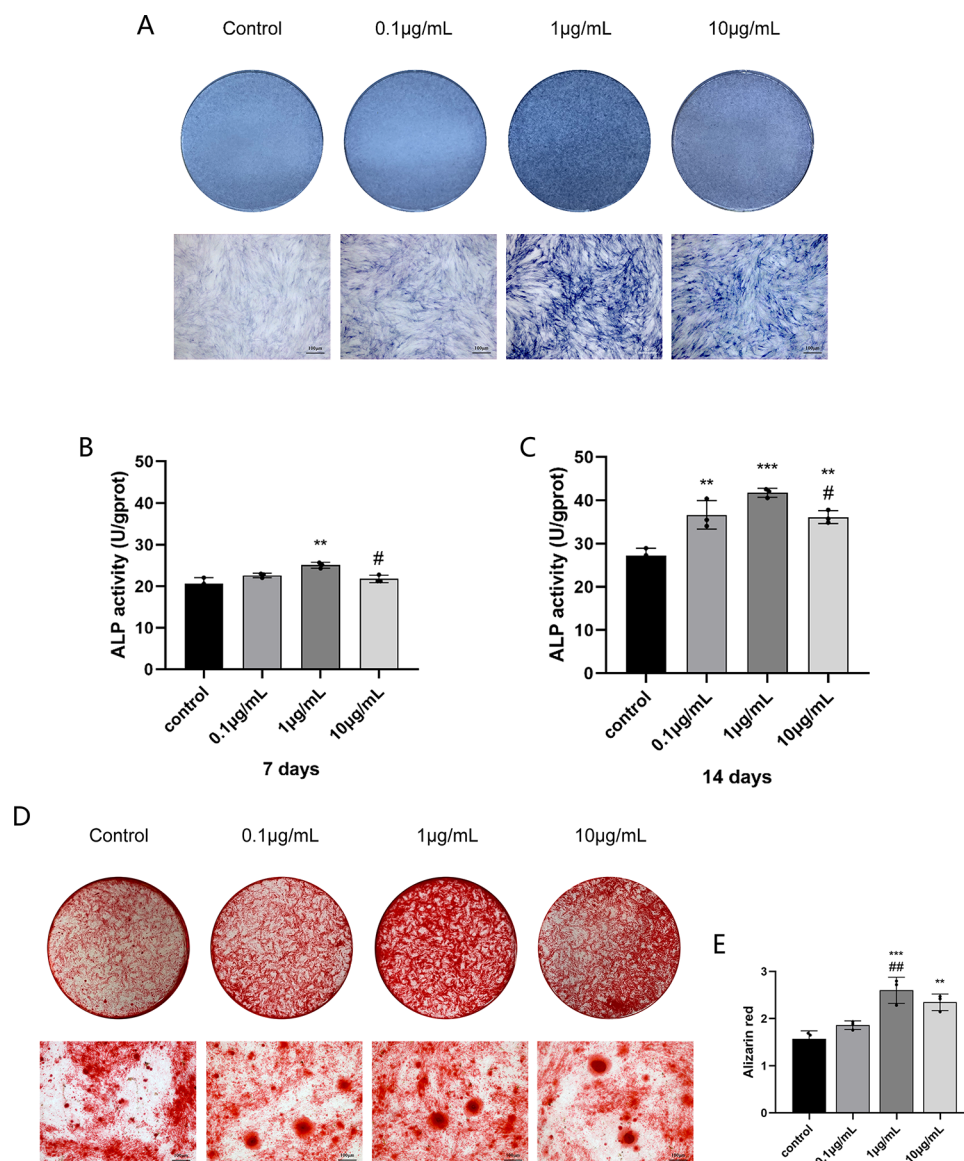


**Figure 5.** DPSCs were cultured in odontogenic induction medium containing different concentrations (0, 0.1, 1, and 10  $\mu\text{g}/\text{mL}$ ) of GOQDs. (A) Gross appearance and microscopic images of ALP staining,  $\times 50$ ; (B, C) quantitative detection of ALP activity for 7 and 14 days of coculture; (D) gross appearance and microscopic images of Alizarin red staining,  $\times 50$ ; (E) semi-quantitative interpretation of Alizarin red staining (\*\* $p < 0.01$ , and \*\*\* $p < 0.001$  vs the control group; ## $p < 0.01$  vs 0.1  $\mu\text{g}/\text{mL}$  GOQDs;  $\#p < 0.05$  vs 1  $\mu\text{g}/\text{mL}$  GOQDs).

concentration of GOQDs in such a promotional effect is 1  $\mu\text{g}/\text{mL}$  in this study.

**2.7. Inhibitor Treatment.** In order to explore the molecular mechanism of the promotional effect of odontoblastic differentiation caused by GOQDs, we treat DPSCs with compound C, which is an inhibitor of the AMPK pathway, and the carry-over effect was detected by ALP and Alizarin red staining, qRT-PCR and western blotting. The result (Figure 7A–H) indicated that compared with the control group, GOQDs at the concentration of 1  $\mu\text{g}/\text{mL}$  can significantly stimulate the mineralization capacity and ALP activity, as well as the expression levels of odontogenic genes and proteins, of DPSCs with odontogenic incubation. However, after treatment with compound C, such a promotional effect of GOQDs in DPSCs was reversed, which was manifested in the decrease of calcium nodule's deposition and ALP activity, and the reduction of odontoblastic differentiation related genes and protein's expression as well. This indicated that GOQDs can

influence the odontoblastic differentiation of DPSCs through the AMPK signaling pathway.

**2.8. Effects of AMPK/mTOR.** DPSCs were cocultured with OIM, which include different concentrations (0.1, 1, and 10  $\mu\text{g}/\text{mL}$ ) of GOQDs for 14 days, and then western blotting was used to detect the protein activation levels of AMPK and mTOR pathways. According to the result (Figure 8A–C), after coculturing with GOQDs at low concentrations (0.1, 1, and 10  $\mu\text{g}/\text{mL}$ ), the expression level of phosphorylated AMPK increased, while the expression level of phosphorylated mTOR decreased, which suggested that GOQDs at low concentration can activate the AMPK pathway and inhibit the mTOR pathway in DPSCs. In this study, the optimum concentration of GOQDs for activating the AMPK pathway while inhibiting the mTOR pathway was 1  $\mu\text{g}/\text{mL}$ . This result was consistent with the aforementioned optimum concentration of GOQDs for promoting the odontoblastic differentiation.

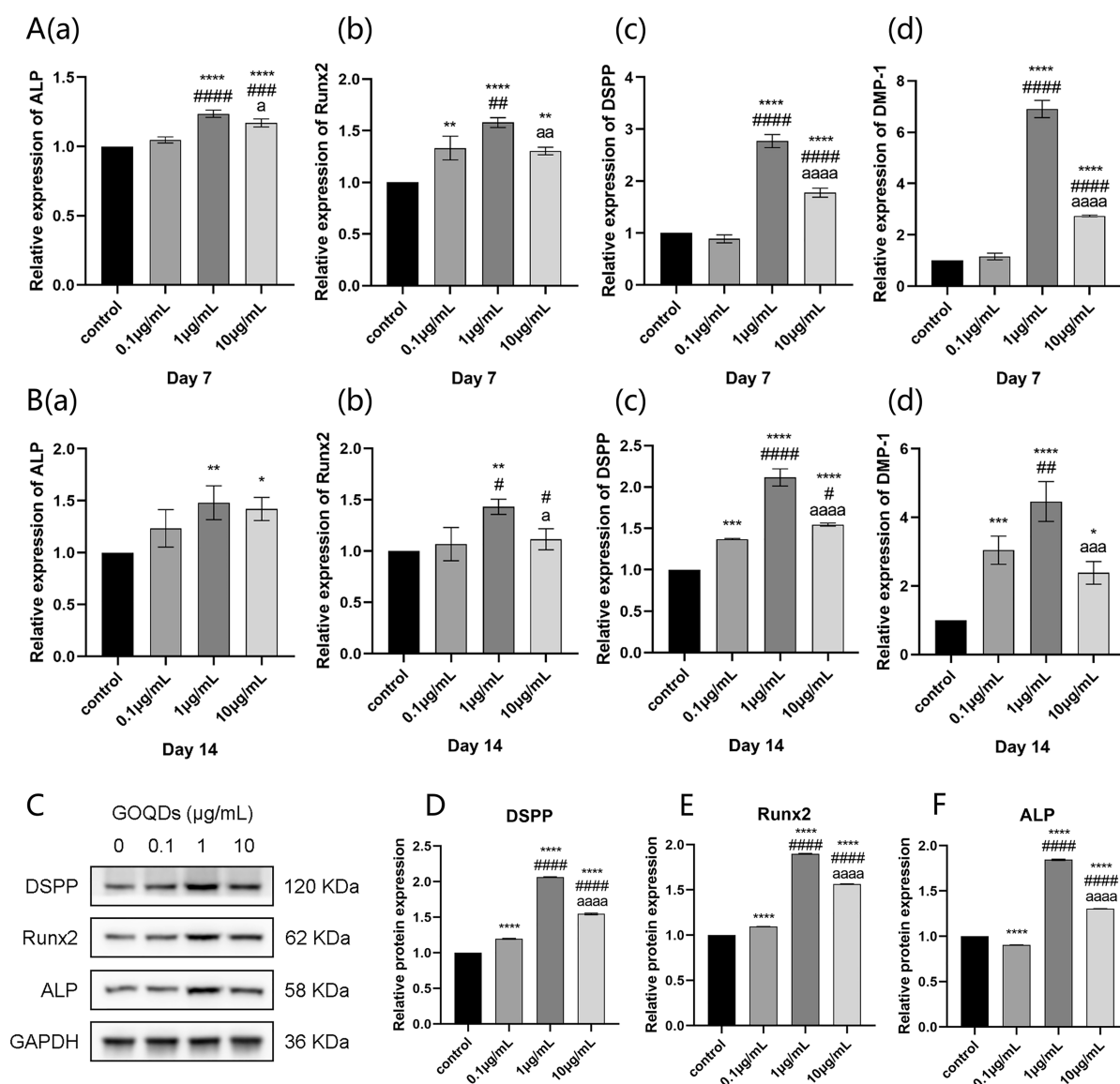


**Figure 6.** qRT-PCR and western blotting analyses of the expression levels of odontogenic proteins and genes of DPSCs cocultured with GOQDs at different concentrations. (A) Expression levels of odontogenic genes of 7 days' coculture tested by qRT-PCR; (B) expression levels of odontogenic genes of 14 days of coculture tested by qRT-PCR; (C) expression levels of odontogenic proteins of 14 days of coculture analyzed by western blotting; (D–F) quantitative analyses of western blotting (\* $p < 0.05$ , \*\* $p < 0.01$ , \*\*\* $p < 0.001$ , and \*\*\*\* $p < 0.0001$  vs the control group; # $p < 0.05$ , ## $p < 0.01$ , ### $p < 0.001$ , and #### $p < 0.0001$  vs 0.1  $\mu\text{g/mL}$  GOQDs;  $a_p < 0.05$ ,  $aa_p < 0.01$ ,  $aaa_p < 0.001$ , and  $aaaa_p < 0.0001$  vs 1  $\mu\text{g/mL}$  GOQDs).

### 3. DISCUSSION

Quantum dots exhibit great potential in the biomedical field. In the current research, semiconductor quantum dots stand out in the field of bioimaging due to their optical properties. However, there are few studies on the impact of quantum dots on the behavior of stem cells. Some studies have proved that GQDs and their derivatives can affect the self-renewal and cell differentiation of MSCs. Among these, studies on osteoblastic differentiation of MSCs are the most common. Qiu et al.<sup>17</sup> proved that GQDs at an appropriate concentration can promote the expression of osteogenesis related genes and proteins in BMSCs. Han et al.<sup>36</sup> proved that GQD based on adenosine and aspirin can promote osteogenic differentiation of BMSCs. Our previous research also proved that GOQDs can promote osteogenic differentiation of SHEDs<sup>18</sup> and BMSCs.<sup>19</sup> Because of the similarity in mineralization between

osteogenic and odontogenic differentiation, it is reasonable to speculate that GQDs and their derivatives can also promote the odontogenic differentiation of stem cells.

However, most studies have not explored the optimal concentration of GQDs and their derivatives for application. At the cellular level, the overall toxicity of quantum dots appears at the threshold concentration.<sup>37</sup> Compared with differentiated cells, stem cells are more resistant to quantum dots. In terms of the concentration of GQDs, the toxicity of GQDs increases with the increase of concentration. With the increase of concentration, GQDs can aggregate into a larger cluster and then lead to the formation of pores in the lipid membrane.<sup>38</sup> In a cytotoxicity study of graphite nanoparticles, cell viability decreased in a concentration-dependent manner (10–100  $\mu\text{g/mL}$ ) and had a steeply decrease at concentrations greater than 30  $\mu\text{g/mL}$ .<sup>39</sup> This indicated that graphite nanoparticles have

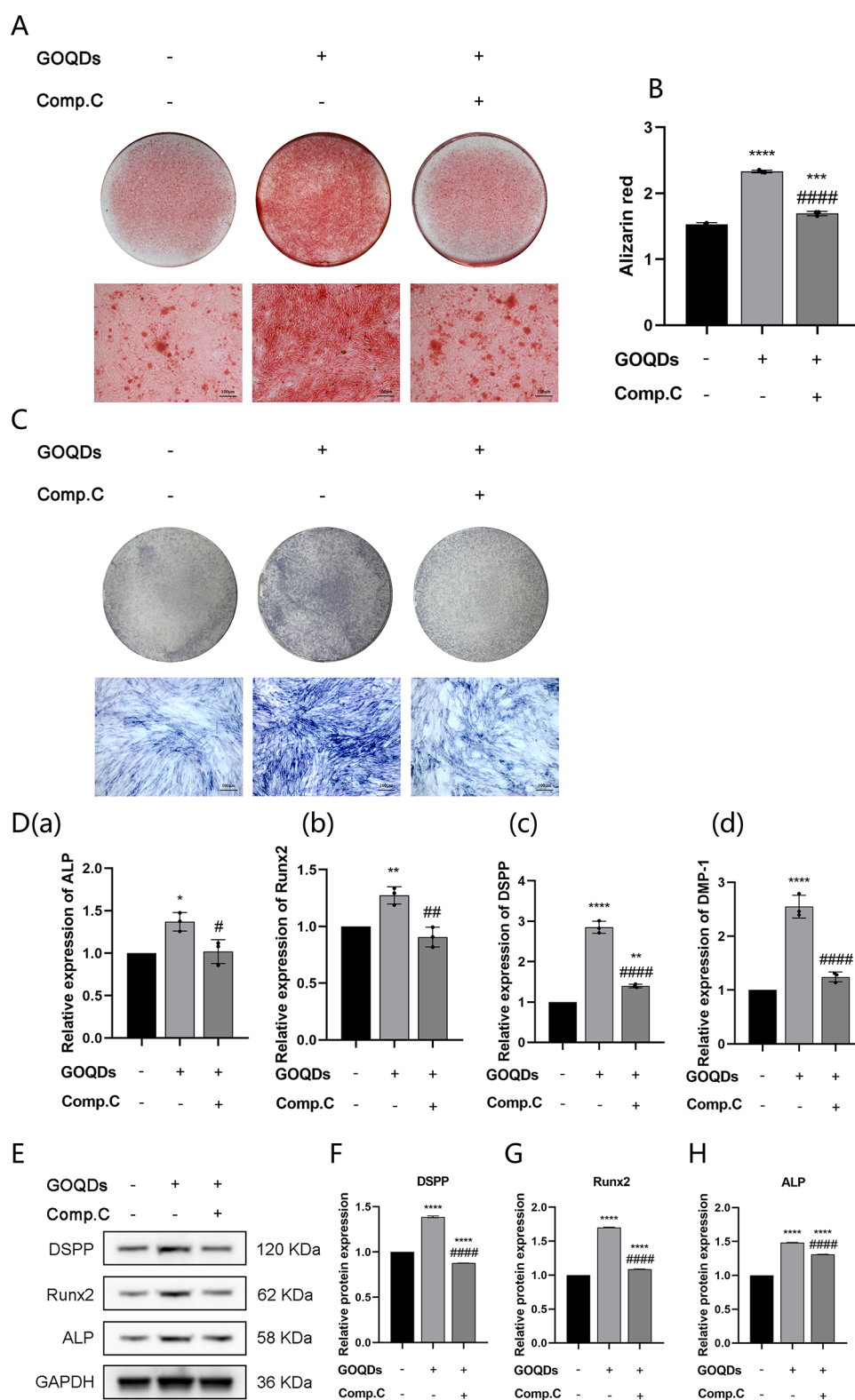


**Figure 7.** Effect of compound C. (A) Gross appearance and microscopic images of Alizarin red staining,  $\times 50$ ; (B) semi-quantitative interpretation of Alizarin red staining; (C) gross appearance and microscopic images of ALP staining,  $\times 50$ ; (D) expression levels of odontogenic genes tested by qRT-PCR; (E–H) expression levels of odontogenic proteins analyzed by western blotting (\* $p < 0.05$ , \*\* $p < 0.01$ , and \*\*\*\* $p < 0.0001$  vs the control group; # $p < 0.05$ , ## $p < 0.01$ , and #### $p < 0.0001$  vs GOQDs (+) Comp.C(–) group).

significant concentration-dependent toxicity in vitro, and 30  $\mu\text{g}/\text{mL}$  might be the threshold concentration. Therefore, according to the expected application of quantum dots, the optimal concentration range must be defined to obtain the

expected effect of the study. In this study, we analyzed the effects of GOQDs at different concentrations on the proliferation of DPSCs. The results of the CCK-8 assay show that GOQDs have dose-dependent toxicity to DPSCs.

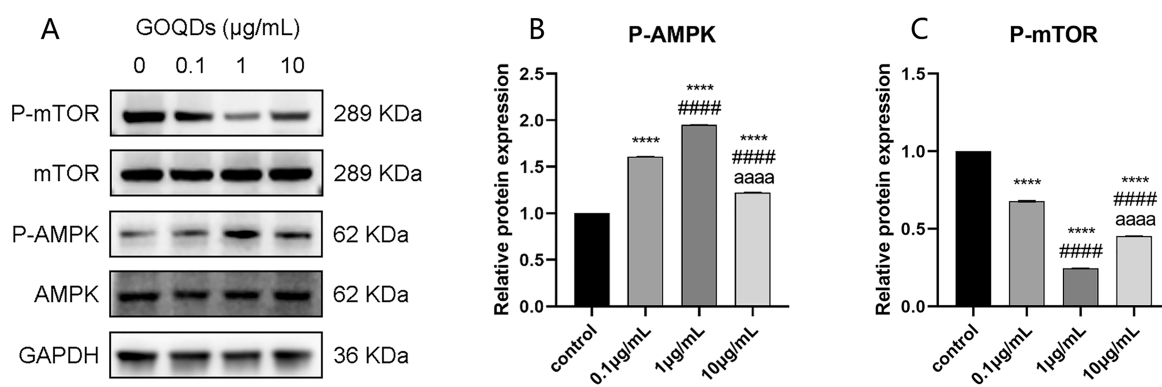


**Figure 8.** Protein activation levels of AMPK and mTOR pathways. (A–C) Protein expression levels of AMPK/mTOR pathway analyzed by western blotting (\*\*\*\* $p < 0.0001$  vs the control group; #### $p < 0.0001$  vs 0.1  $\mu\text{g/mL}$  GOQDs; aaaa $p < 0.0001$  vs 1  $\mu\text{g/mL}$  GOQDs).

Compared with the control group, when the concentration of GOQDs reached 50  $\mu\text{g/mL}$ , the proliferation activity of DPSCs was inhibited. However, when the concentration of GOQDs was 0.1, 1, or 10  $\mu\text{g/mL}$ , GOQDs can significantly increase the proliferation activity of DPSCs. 50  $\mu\text{g/mL}$  seems to be a common threshold concentration for quantum dots to exhibit cytotoxicity. In Wang et al.'s study<sup>40</sup> on the enhancement of osteogenic differentiation of BMSC caused by GQDs, the concentration range of quantum dots is 0.5–50  $\mu\text{g/mL}$ . When the concentration of GQDs is 50  $\mu\text{g/mL}$ , cell viability was slightly inhibited after coculturing for 72 h. Therefore, they believe that the safe treatment concentration should be less than 50  $\mu\text{g/mL}$ . Another study<sup>17</sup> also showed that 50  $\mu\text{g/mL}$  GQDs can start to inhibit the proliferation of MSCs, which is consistent with the results of our study. Different concentrations of GOQDs lead to different cell proliferative ability, which may be attributed to the dual behaviors of GOQDs based on concentration:<sup>8</sup> in an appropriate concentration range, GOQDs can promote cell survival by reducing intracellular ROS, stimulating the synthesis of growth promoting factors and degrading toxic proteins;<sup>10</sup> If GOQDs exceed this concentration range, these nanoparticles will exhibit cytotoxicity of quantum dots.<sup>41</sup> Nanoparticles at an excessive concentration would accumulate and interact with the surrounding cells, granulating the cellular microenvironment and increasing the risk of cellular structural damage.

Attributed to the nanoscale size of GOQDs, these nanoparticles exhibit a distinct physicochemical characteristic from GO, including penetrating across cell barriers and then directly producing intracellular effects.<sup>42</sup> The cellular uptake of quantum dots is a process of active transport, and clathrin-mediated endocytosis is possibly the dominant way for the internalization of quantum dots.<sup>43</sup> The result of cellular immunofluorescence staining showed that, after coculture, GOQDs could aggregate in DPSCs and emit blue fluorescence under 405 nm of excitation wavelength due to photoluminescence features. In addition, the actin filaments of DPSCs treated with 0.1, 1, or 10  $\mu\text{g/mL}$  GOQDs exhibited normal spindle-like morphology, indicating that GOQDs did not affect the normal cell morphology of DPSCs within this concentration range.

Alkaline phosphatase (ALP) is an extracellular enzyme that releases phosphate for mineralization at the stage of cell differentiation, which is closely related to the secretory activity of cells. Regarded as an early marker of osteogenic and odontoblastic differentiation, ALP usually significantly ex-

presses after 1 week of induction.<sup>44</sup> The result of the ALP activity assay and ALP staining showed that, after coculturing with GOQDs, DPSCs exhibited higher ALP expression than those in the control group, and DPSCs treated with 1  $\mu\text{g/mL}$  GOQDs had the highest ALP activity. Alizarin red staining and the semi-quantitative interpretation can detect the calcium deposits content in the extracellular matrix. The results of these experiments were consistent with the results of the ALP activity assay and ALP staining, indicating that 1  $\mu\text{g/mL}$  GOQDs can promote the formation of calcium nodules in extracellular matrix.

Dentin sialophosphoprotein (DSPP) and dentin matrix protein-1 (DMP-1) are positive regulators of hard tissue mineralization,<sup>45</sup> which play significant roles in early odontoblast differentiation and later dentin mineralization. DPSS can encode two dentin matrix proteins, including dentin sialoprotein (DSP) and dentin phosphoprotein (DPP). DSP is the regulator of initiation of dentin mineralization, while DPP is the regulator of mineralized dentin maturation.<sup>44</sup> Therefore, the increased expression of DSPP and its cleavage products confirmed odontoblastic differentiation of DPSCs, and the expression of DSPP in odontoblasts and dentin was 400 times higher than that in osteoblasts and bone tissue.<sup>46</sup> DMP-1 is an extracellular matrix protein that can induce the deposition of mineral particles along the collagen fibril axis and produce a marked effect in regulating dentin mineralization.<sup>47</sup> Runx2 is a specific transcription factor that regulates the differentiation of mesenchymal stem cells, and it is closely related to the differentiation of odontoblasts. The expression of Runx2 has temporospatial characteristic for its high expression at the early stage of odontoblast differentiation.<sup>48</sup> The results of qRT-PCR and western blotting showed that, after coculturing with GOQDs, the expression levels of odontoblastic differentiation-related genes and proteins in DPSCs were significantly increased, and this increase was affected by the concentration of GOQDs. Compared with other concentrations of GOQDs, 1  $\mu\text{g/mL}$  GOQDs have a stronger ability to promote odontoblast differentiation, which was consistent with the results of the previous ALP related experiments and Alizarin red staining. However, in the previous experiment of our research group, the optimal concentration of GOQDs to promote osteogenic differentiation of BMSCs and SHEDs were 0.1<sup>19</sup> and 10  $\mu\text{g/mL}$ .<sup>18</sup> This discrepancy may be due to the different sensitivity of different cell types to the concentration of quantum dots.

Intracellular nanoparticles are not only degraded by the endolysosomal pathway but also encapsulated by autophago-

somes, which would result in degrading by the autolysosomal pathway. Autophagy caused by nanoparticles may be a cellular defense mechanism to against nanoparticles,<sup>10</sup> for it has a protective effect on the toxicity of quantum dots.<sup>49</sup> The study by Wang et al.<sup>50</sup> showed that oxidative stress is triggered by the generation of ROS during the process of carbon dots promoting osteogenic differentiation. When studying the mineralization of DPSCs induced by GOQDs, Li et al.<sup>51</sup> also found the involvement of ROS, which suggested the occurrence of autophagy. During the process of cell differentiation, unnecessary proteins can be degraded by autophagy to provide zymolyte for the synthesis of new morphogenesis related proteins. Autophagy is regulated by nutrient sensors, AMPK and mTOR, and coordinates physiological conditions and environmental stress of cells in the form of signal pathways.<sup>26</sup> The complex protein network composed by AMPK and mTOR is mainly regulated by rapid and reversible post-translational modifications, such as phosphorylation.<sup>52</sup> Phosphorylated AMPK can induce autophagy by inhibiting mTOR.<sup>34</sup> Unc-51-like kinase 1 (Ulk1) is the main checkpoint regulating autophagy initiation.<sup>53</sup> mTOR inhibited by AMPK can eliminate the phosphorylation inhibition of Ulk1 and then induce the combination of Ulk1 and AMPK, which is a main mechanism of autophagy induced by AMPK. AMPK and mTOR synergistically regulate Ulk1 to control autophagy, which means that the dynamic balance of autophagy depends on the signaling triad formed by a transient feedback mechanism of AMPK, mTOR, and Ulk1.<sup>54</sup> Compound C (also known as dorsomorphin) is a selective and competitive AMPK inhibitor with cell permeability, which is widely used in cell-based, biochemical, and in vivo assays.<sup>55</sup> In this study, compared with the control group, DPSCs cocultured with GOQDs exhibited better ability of odontoblast differentiation, accompanied by activation of the AMPK pathway and inhibition of the mTOR pathway, indicating that GOQDs can regulate the odontoblast differentiation ability of DPSCs through the AMPK/mTOR pathway. Studies have shown that the process of nanoparticle cellular internalization may affect the recruitment/activation of AKT localized at the cell membrane, thereby altering its ability to activate mTOR. Meanwhile, the internalized nanoparticles could further affect the activation of mTOR by preventing the recruitment of mTOR to the lysosomal membrane.<sup>56</sup> This may explain the reason why GOQDs lead to mTOR pathway inhibition in this experiment. Between all the concentration groups, 1  $\mu\text{g}/\text{mL}$  GOQDs showed the strongest effect of odontogenic induction. After the application of the AMPK inhibitor compound C, the promotion of odontoblast differentiation caused by 1  $\mu\text{g}/\text{mL}$  GOQDs was partially reversed.

Based on these results, we demonstrated that the internalization of GOQDs at an appropriate concentration could activate AMPK and inhibit mTOR, thereby promoting odontoblastic differentiation of DPSCs. The odontoblastic differentiation effect of GOQDs showed a significant concentration dependence, and 1  $\mu\text{g}/\text{mL}$  was the optimum concentration for this promoting effect in this experiment. When the concentration of GOQDs was 50  $\mu\text{g}/\text{mL}$ , it showed an inhibitory effect on the cell viability of DPSCs. However, in this study, whether cellular defensive autophagy against GOQDs occurs with the activation of the AMPK/mTOR signaling pathway requires further investigation.

## 4. MATERIALS AND METHODS

**4.1. Characterization of GOQDs.** GOQDs were provided by Nanjing Xianfeng (Nanjing XFANO Materials, China). The concentration of GOQDs colloid was 1 mg/mL, and the solvent is water. The size and nanomorphology of GOQDs were detected by transmission electron microscopy (TEM; FEI Tecnai G2 Spirit, Hillsboro, OR, USA). The composition of GOQDs was characterized by X-ray photoelectron spectroscopy (XPS).

**4.2. Isolation and Characterization of DPSCs.** DPSCs were isolated from intact third molars extracted from clinical patients (20–30 years old), and these caries-free third molars were extracted for being impacted or orthodontic treatment. Ethics Committee approval was provided by the School of Stomatology, Sun Yat-sen University. The teeth were stored in precooled phosphate-buffered saline (PBS; Hyclone, Logan, UT, USA) with 1% penicillin/streptomycin (P/S; Gibco, Thermo Fisher Scientific, Inc., GrandIsland, NY, USA) before being taken to the laboratory. After cleaning the surface of the teeth in clean bench, pulp tissue was extracted from teeth split longitudinally. The pulp tissue was sheared into 1 mm<sup>3</sup> pieces and digested with 1:1 3 g/L collagenase type I (Sigma-Aldrich, St. Louis, MO, USA) and 4 g/L dispase (Roche, Basel, Switzerland) at 37 °C for 30 min. The discrete cells were resuspended in Dulbecco's modified Eagle's medium (DMEM; Gibco), which included 20% fetal bovine serum (FBS; Gibco), and then cultured in 37 °C and 5% CO<sub>2</sub> incubator. The medium was changed every 3 days.

The cell morphology of primary and third-passage DPSCs was observed by an inverted microscope (Zeiss, Oberkochen, Germany). Adipogenic induction medium (Cyagen Biosciences, China) was used to induce adipogenic differentiation of DPSCs. After 21 days of adipogenic induction, Oil red O staining was applied to evaluate the formation of lipid droplet. Osteogenic induction medium [DMEM with 10% FBS, 1% P/S, 0.1  $\mu\text{M}$  dexamethasone (Sigma-Aldrich), 10 mM  $\beta$ -glycerophosphate (Sigma-Aldrich), and 50  $\mu\text{M}$  ascorbic acid (Sigma-Aldrich)] was applied to induce osteogenic differentiation of DPSCs. After 14 days of osteogenic induction, Alizarin red staining was used to evaluate the deposition of calcium nodules. Flow cytometry was performed with the Beckman Coulter CytoFlex system, and the characterization of DPSCs was assessment by CD34, CD44, CD45, CD73, CD90, and CD105.

**4.3. Proliferation Assay.** DPSCs were seeded in 96-well plates at a density of  $5 \times 10^3$  per well. After 24 h, the cells adhered and the growth state was stable, and then the medium was changed to the medium containing GOQDs. The cells were cocultured with medium (DMEM, 10% FBS and 1% P/S), which include different concentrations (0, 0.1, 1, 10, and 50  $\mu\text{g}/\text{mL}$ ) of GOQDs. The medium was changed every 2 days. Cell proliferation of DPSCs was detected by a Cell Counting Kit-8 (CCK-8; Beyotime, China). After 1, 3, 5, and 7 days of coculture, the medium was changed into 100  $\mu\text{L}$  DMEM with 10  $\mu\text{L}$  of CCK-8, and then well plates were incubated at 37 °C and CO<sub>2</sub> for 1 h. The OD value of each well was detected by a microplate reader (Tecan, Männedorf, Switzerland) at a wavelength of 450 nm.

**4.4. Live Cell Imaging.** DPSCs were plated on laser-scanning confocal petri dish at  $1 \times 10^4$  cells per dish. DPSCs were cocultured with a medium, which include different concentrations (0, 0.1, 1, and 10  $\mu\text{g}/\text{mL}$ ) of GOQDs after cell

attachment. After 72 h, DPSCs were rinsed with PBS and fixed with 4% paraformaldehyde for 30 min. The cells were treated with 0.1% Triton X-100 for 15 min, and then 100  $\mu$ L of phalloidin was used for cytoskeleton staining. The morphology of DPSCs was observed by confocal laser scanning microscopy (Olympus, Japan).

**4.5. ALP Activity Assay and ALP Staining.** The odontogenic induction medium (OIM) is DMEM with 10% FBS, 1% P/S, 0.1  $\mu$ M dexamethasone (Sigma-Aldrich), 10 mM  $\beta$ -glycerophosphate (Sigma-Aldrich), and 50  $\mu$ M ascorbic acid (Sigma-Aldrich). DPSCs were seeded in 6-well plates at a density of  $2 \times 10^5$  per well and then cocultured with OIM, which include different concentrations (0, 0.1, 1, and 10  $\mu$ g/mL) of GOQDs after cell attachment. The medium was changed every 2 days. For ALP activity determination, the ALP assay kit (Nanjing Jiancheng Bioengineering Institute, China) was applied after 7 and 14 days of coculture. ALP staining was performed by the BCIP/NBT Alkaline Phosphatase Color Development Kit (Beyotime) after 7 days of coculture.

**4.6. Alizarin Red Staining.** DPSCs were seeded in 6-well plates at a density of  $2 \times 10^5$  per well and then cocultured with OIM, which include different concentrations (0, 0.1, 1, and 10  $\mu$ g/mL) of GOQDs for 14 days after cell attachment. The medium was changed every 2 days. The cells were fixed by 4% paraformaldehyde for 30 min and then were dyed by Alizarin red (Cyagen Biosciences) for 30 min. The photographs of calcium nodules were taken by an inverted fluorescence microscope (Zeiss). For semi-quantitative interpretation, 10% cetylpyridinium chloride (Sigma) was added into each well, and the OD value was detected at a wavelength of 562 nm.

**4.7. qRT-PCR.** The cell seeding density was the same as above. After coculturing with OIM, which include different concentrations (0, 0.1, 1, and 10  $\mu$ g/mL) of GOQDs for 7 and 14 days, total RNA was extracted by the RNA-Quick Purification Kit (YiShan Biotech, China). Complementary DNA was obtained through mRNA by PrimeScript RT Master Mix (Takara Bio Inc., Japan). The expression of odontogenic related genes (ALP, Runx2, DSPP, and DMP-1) were quantified by qRT-PCR, and GAPDH was regarded as the internal control. The primer sequences are shown in Table 1.

**Table 1. Primer Sequence Used in qRT-PCR**

gene	primer	sequence
DSPP	forward	5'-CAACCATAGAGAAAGCAAACGCG-3'
	reverse	5'-TTTCTGTTGCCACTGCTGGGAC-3'
DMP-1	forward	5'-GAGCAGTGAGTCATCAGAAGGC-3'
	reverse	5'-GAGAAGCCACCAGCTAGCCTAT-3'
ALP	forward	5'-CCTCCTCGGAAGACACTCTG-3'
	reverse	5'-GCAGTGAAGGGCTTCTTGTC-3'
Runx2	forward	5'-CCACTGAACCAAAAAGAAATCCC-3'
	reverse	5'-GAAAACAACACATAGCCAAACGC-3'
GAPDH	forward	5'-TCTCCTCTGACTTCAACAGCGACA-3'
	reverse	5'-CCCTGTTGCTGTAGCCAAATTCGT-3'

**4.8. Western Blotting.** The cell seeding density was the same as above. After coculturing with OIM, which include different concentrations (0, 0.1, 1, and 10  $\mu$ g/mL) of GOQDs for 14 days, RIPA was applied to lyse DPSCs and extract proteins. The concentration of proteins was detected by the BCA assay kit (CWBIO, China). The proteins separated by 10% SDS-PAGE (GenSpirt, China) were transferred to polyvinylidene fluoride (PVDF) membranes (Millipore,

USA) and then were blocked by Tris-buffered saline with Tween (TBST) with 5% skimmed milk for 1 h. The PVDF membranes were incubated with primary antibodies against ALP, Runx2, DSPP, and GAPDH at 4  $^{\circ}$ C for 18 h, after which the membranes were rinsed by TBST and incubated with secondary antibody for 1 h in room temperature. The enhanced chemiluminescent (ECL) detection system (Millipore) was applied to detect the immunoblots, and ImageJ software (National Institutes of Health, Bethesda, MD, USA) was used for quantification.

**4.9. Inhibitor Treatment.** DPSCs were plated on 6-well plates at  $2 \times 10^5$  cells per well. DPSCs were divided into three groups: control group (DPSCs cultured in OIM), GOQDs group (DPSCs cultured in OIM with 1  $\mu$ g/mL GOQDs), and Comp.C group (DPSCs cultured in OIM with 1  $\mu$ g/mL GOQDs after treatment with 10  $\mu$ M compound C for 4 h). The cells were cultured respectively as the above methods for 7 and 14 days, and the effect of compound C was testified by ALP staining, Alizarin red staining, qRT-PCR, and western blotting.

**4.10. Effects of AMPK/mTOR.** DPSCs were plated on 6-well plates at  $2 \times 10^5$  cells per well and then cocultured with OIM, which include different concentrations (0, 0.1, 1, and 10  $\mu$ g/mL) of GOQDs for 14 days after cell attachment. Except for the application of 4–12% SDS-PAGE (GenSpirt), the methods of protein extraction and western blotting were the same as above. AMPK/mTOR pathway protein expression was indicated by western blotting.

**4.11. Statistical Analysis.** The presented data are shown as means  $\pm$  standard deviations. Significant differences between and within groups were assessed by *t*-test and one-way analysis of variance (ANOVA). *P* < 0.05 was regarded as a significant difference. SPSS 20.0 software (SPSS Inc., Chicago, Illinois, USA) was used for statistical analyses.

## 5. CONCLUSIONS

The cellular uptake of GOQDs in a proper concentration range promotes proliferation and odontoblastic differentiation of DPSCs, and the AMPK/mTOR signaling pathway is involved in this promotion. The odontoblastic differentiation effect of GOQDs showed a significant concentration dependence, and the optimum concentration of GOQDs in such facilitation is 1  $\mu$ g/mL in this study.

## AUTHOR INFORMATION

### Corresponding Authors

**Duoling Xu** – Hospital of Stomatology, Guangdong Provincial Key Laboratory of Stomatology, Guanghua School of Stomatology, Sun Yat-sen University, Guangzhou 510055, China; [orcid.org/0000-0003-1657-8723](https://orcid.org/0000-0003-1657-8723); Email: [xudling@mail2.sysu.edu.cn](mailto:xudling@mail2.sysu.edu.cn)

**Wei Zhao** – Hospital of Stomatology, Guangdong Provincial Key Laboratory of Stomatology, Guanghua School of Stomatology, Sun Yat-sen University, Guangzhou 510055, China; Email: [zhaowei3@mail.sysu.edu.cn](mailto:zhaowei3@mail.sysu.edu.cn)

### Authors

**Ling Lin** – Hospital of Stomatology, Guangdong Provincial Key Laboratory of Stomatology, Guanghua School of Stomatology, Sun Yat-sen University, Guangzhou 510055, China; [orcid.org/0000-0002-6095-6501](https://orcid.org/0000-0002-6095-6501)

**Yexin Zheng** – Hospital of Stomatology, Guangdong Provincial Key Laboratory of Stomatology, Guanghua School

of Stomatology, Sun Yat-sen University, Guangzhou 510055, China

**Chao Wang** – Hospital of Stomatology, Guangdong Provincial Key Laboratory of Stomatology, Guanghua School of Stomatology, Sun Yat-sen University, Guangzhou 510055, China; [orcid.org/0000-0001-8384-0977](https://orcid.org/0000-0001-8384-0977)

**Pei Li** – Hospital of Stomatology, Guangdong Provincial Key Laboratory of Stomatology, Guanghua School of Stomatology, Sun Yat-sen University, Guangzhou 510055, China

Complete contact information is available at:  
<https://pubs.acs.org/10.1021/acsomega.2c06508>

## Notes

The authors declare no competing financial interest.

## ACKNOWLEDGMENTS

This work was financially supported by the National Natural Science Foundation of China (nos. 81974146) and the Key Technologies R&D Program of Guangdong Province (2020B1111490004).

## REFERENCES

- (1) Bjørndal, L.; Simon, S.; Tomson, P. L.; Duncan, H. F. Management of deep caries and the exposed pulp. *Int. Endod. J.* **2019**, *52*, 949–973.
- (2) Whitehouse, L. L. E.; Thomson, N. H.; Do, T.; Feichtinger, G. A. Bioactive molecules for regenerative pulp capping. *Eur. Cell Mater.* **2021**, *42*, 415–437.
- (3) Kunert, M.; Lukomska-Szymanska, M. Bio-Inductive Materials in Direct and Indirect Pulp Capping-A Review Article. *Materials* **2020**, *13*, 1204.
- (4) da Rosa, W. L. O.; Piva, E.; da Silva, A. F. Disclosing the physiology of pulp tissue for vital pulp therapy. *Int. Endod. J.* **2018**, *51*, 829–846.
- (5) Zhang, C.; Xie, B.; Zou, Y.; Zhu, D.; Lei, L.; Zhao, D.; Nie, H. Zero-dimensional, one-dimensional, two-dimensional and three-dimensional biomaterials for cell fate regulation. *Adv. Drug Delivery Rev.* **2018**, *132*, 33–56.
- (6) Majood, M.; Garg, P.; Chaurasia, R.; Agarwal, A.; Mohanty, S.; Mukherjee, M. Carbon Quantum Dots for Stem Cell Imaging and Deciding the Fate of Stem Cell Differentiation. *ACS Omega* **2022**, *7*, 28685–28693.
- (7) Cheng, Z.; Li, M.; Dey, R.; Chen, Y. Nanomaterials for cancer therapy: current progress and perspectives. *J. Hematol. Oncol.* **2021**, *14*, 85.
- (8) Mohammadinejad, R.; Moosavi, M. A.; Tavakol, S.; Vardar, D. O.; Hosseini, A.; Rahmati, M.; Dini, L.; Hussain, S.; Mandegary, A.; Klionsky, D. J. Necrotic, apoptotic and autophagic cell fates triggered by nanoparticles. *Autophagy* **2019**, *15*, 4–33.
- (9) Napi, M. L. M.; Sultan, S. M.; Ismail, R.; How, K. W.; Ahmad, M. K. Electrochemical-Based Biosensors on Different Zinc Oxide Nanostructures: A Review. *Materials* **2019**, *12*, 2985.
- (10) Guo, L.; He, N.; Zhao, Y.; Liu, T.; Deng, Y. Autophagy Modulated by Inorganic Nanomaterials. *Theranostics* **2020**, *10*, 3206–3222.
- (11) Asgari, V.; Landarani-Isfahani, A.; Salehi, H.; Amirpour, N.; Hashemibeni, B.; Rezaei, S.; Bahramian, H. The Story of Nanoparticles in Differentiation of Stem Cells into Neural Cells. *Neurochem. Res.* **2019**, *44*, 2695–2707.
- (12) Geng, H.; Qiu, J.; Zhu, H.; Liu, X. Achieving stem cell imaging and osteogenic differentiation by using nitrogen doped graphene quantum dots. *J. Mater. Sci. Mater. Med.* **2018**, *29*, 85.
- (13) Henna, T. K.; Pramod, K. Graphene quantum dots redefine nanobiomedicine. *Mater. Sci. Eng. C Mater. Biol. Appl.* **2020**, *110*, 110651.
- (14) Ristic, B. Z.; Milenkovic, M. M.; Dakic, I. R.; Todorovic-Markovic, B. M.; Milosavljevic, M. S.; Budimir, M. D.; Paunovic, V. G.; Dramicanin, M. D.; Markovic, Z. M.; Trajkovic, V. S. Photodynamic antibacterial effect of graphene quantum dots. *Biomaterials* **2014**, *35*, 4428–4435.
- (15) Zeng, Z.; Yu, D.; He, Z.; Liu, J.; Xiao, F. X.; Zhang, Y.; Wang, R.; Bhattacharyya, D.; Tan, T. T. Graphene Oxide Quantum Dots Covalently Functionalized PVDF Membrane with Significantly-Enhanced Bactericidal and Antibiofouling Performances. *Sci. Rep.* **2016**, *6*, 20142.
- (16) Sun, H.; Gao, N.; Dong, K.; Ren, J.; Qu, X. Graphene quantum dots-band-aids used for wound disinfection. *ACS Nano* **2014**, *8*, 6202–6210.
- (17) Qiu, J.; Li, D.; Mou, X.; Li, J.; Guo, W.; Wang, S.; Yu, X.; Ma, B.; Zhang, S.; Tang, W.; Sang, Y.; Gil, P. R.; Liu, H. Effects of Graphene Quantum Dots on the Self-Renewal and Differentiation of Mesenchymal Stem Cells. *Adv. Healthcare Mater.* **2016**, *5*, 702–710.
- (18) Yang, X.; Zhao, Q.; Chen, J.; Liu, J.; Lin, J.; Lu, J.; Li, W.; Yu, D.; Zhao, W. Graphene Oxide Quantum Dots Promote Osteogenic Differentiation of Stem Cells from Human Exfoliated Deciduous Teeth via the Wnt/beta-Catenin Signaling Pathway. *Stem Cells Int.* **2021**, *2021*, 8876745.
- (19) Xu, D.; Wang, C.; Wu, J.; Fu, Y.; Li, S.; Hou, W.; Lin, L.; Li, P.; Yu, D.; Zhao, W. Effects of Low-Concentration Graphene Oxide Quantum Dots on Improving the Proliferation and Differentiation Ability of Bone Marrow Mesenchymal Stem Cells through the Wnt/ $\beta$ -Catenin Signaling Pathway. *ACS Omega* **2022**, *7*, 13546–13556.
- (20) Huang, D.; Zhou, H.; Gao, J. Nanoparticles modulate autophagic effect in a dispersity-dependent manner. *Sci. Rep.* **2015**, *5*, 14361.
- (21) Gao, Y.; Zhang, T. The Application of Nanomaterials in Cell Autophagy. *Curr. Stem Cell Res. Ther.* **2021**, *16*, 23–35.
- (22) Wei, T.; Zhang, T.; Tang, M. An overview of quantum dots-induced immunotoxicity and the underlying mechanisms. *Environ. Pollut.* **2022**, *311*, No. 119865.
- (23) Sun, A.; Mu, L.; Hu, X. Graphene Oxide Quantum Dots as Novel Nanozymes for Alcohol Intoxication. *ACS Appl. Mater. Interfaces* **2017**, *9*, 12241–12252.
- (24) Revuelta, M.; Matheu, A. Autophagy in stem cell aging. *Aging Cell* **2017**, *16*, 912–915.
- (25) Adelipour, M.; Saleth, L. R.; Ghavami, S.; Alagarsamy, K. N.; Dhingra, S.; Allameh, A. The role of autophagy in the metabolism and differentiation of stem cells. *Biochim. Biophys. Acta, Mol. Basis Dis.* **1868**, 2022, No. 166412.
- (26) Sotthibundhu, A.; Promjuntuek, W.; Liu, M.; Shen, S.; Noisa, P. Roles of autophagy in controlling stem cell identity: a perspective of self-renewal and differentiation. *Cell Tissue Res.* **2018**, *374*, 205–216.
- (27) Cho, H. S.; Park, S. Y.; Kim, S. M.; Kim, W. J.; Jung, J. Y. Autophagy-Related Protein MAP1LC3C Plays a Crucial Role in Odontogenic Differentiation of Human Dental Pulp Cells. *Tissue Eng. Regen. Med.* **2021**, *18*, 265–277.
- (28) Pei, F.; Wang, H. S.; Chen, Z.; Zhang, L. Autophagy regulates odontoblast differentiation by suppressing NF-kappaB activation in an inflammatory environment. *Cell Death Dis.* **2016**, *7*, No. e2122.
- (29) Saikia, R.; Joseph, J. AMPK: a key regulator of energy stress and calcium-induced autophagy. *J. Mol. Med.* **2021**, *99*, 1539–1551.
- (30) Ristic, B.; Harhaji-Trajkovic, L.; Bosnjak, M.; Dakic, I.; Mijatovic, S.; Trajkovic, V. Modulation of Cancer Cell Autophagic Responses by Graphene-Based Nanomaterials: Molecular Mechanisms and Therapeutic Implications. *Cancers* **2021**, *13*, 4145.
- (31) Tamargo-Gómez, I.; Mariño, G. AMPK: Regulation of Metabolic Dynamics in the Context of Autophagy. *Int. J. Mol. Sci.* **2018**, *19*, 3812.
- (32) Garcia, D.; Shaw, R. J. AMPK: Mechanisms of Cellular Energy Sensing and Restoration of Metabolic Balance. *Mol. Cell* **2017**, *66*, 789–800.
- (33) Weichhart, T. mTOR as Regulator of Lifespan, Aging, and Cellular Senescence: A Mini-Review. *Gerontology* **2018**, *64*, 127–134.

- (34) Zhang, S.; Zhang, R.; Qiao, P.; Ma, X.; Lu, R.; Wang, F.; Li, C.; E, L.; Liu, H. Metformin-Induced MicroRNA-34a-3p Downregulation Alleviates Senescence in Human Dental Pulp Stem Cells by Targeting CAB39 through the AMPK/mTOR Signaling Pathway. *Stem Cells Int.* **2021**, *2021*, 6616240.
- (35) Vidoni, C.; Ferraresi, A.; Secomandi, E.; Vallino, L.; Gardin, C.; Zavan, B.; Mortellaro, C.; Isidoro, C. Autophagy drives osteogenic differentiation of human gingival mesenchymal stem cells. *Cell Commun. Signal* **2019**, *17*, 98.
- (36) Han, Y.; Zhang, F.; Zhang, J.; Shao, D.; Wang, Y.; Li, S.; Lv, S.; Chi, G.; Zhang, M.; Chen, L.; Liu, J. Bioactive carbon dots direct the osteogenic differentiation of human bone marrow mesenchymal stem cells. *Colloids Surf., B* **2019**, *179*, 1–8.
- (37) Filali, S.; Pirot, F.; Miossec, P. Biological Applications and Toxicity Minimization of Semiconductor Quantum Dots. *Trends Biotechnol.* **2020**, *38*, 163–177.
- (38) Liang, L.; Peng, X.; Sun, F.; Kong, Z.; Shen, J. W. A review on the cytotoxicity of graphene quantum dots: from experiment to simulation. *Nanoscale Adv.* **2021**, *3*, 904–917.
- (39) Liao, T. T.; Deng, Q. Y.; Wu, B. J.; Li, S. S.; Li, X.; Wu, J.; Leng, Y. X.; Guo, Y. B.; Huang, N. Dose-dependent cytotoxicity evaluation of graphite nanoparticles for diamond-like carbon film application on artificial joints. *Biomed. Mater.* **2017**, *12*, No. 015018.
- (40) Wang, Z.; Yang, H.; Bai, Y.; Cheng, L.; Zhu, R. rBMSC osteogenic differentiation enhanced by graphene quantum dots loaded with immunomodulatory layered double hydroxide nanoparticles. *Biomed. Mater.* **2022**, *17*, No. 024101.
- (41) Ahmad, J.; Wahab, R.; Siddiqui, M. A.; Saquib, Q.; Al-Khedhairi, A. A. Cytotoxicity and cell death induced by engineered nanostructures (quantum dots and nanoparticles) in human cell lines. *J. Biol. Inorg. Chem.* **2020**, *25*, 325–338.
- (42) Liu, Y. Y.; Chang, Q.; Sun, Z. X.; Liu, J.; Deng, X.; Liu, Y.; Cao, A.; Wang, H. Fate of CdSe/ZnS quantum dots in cells: Endocytosis, translocation and exocytosis. *Colloids Surf., B* **2021**, *208*, No. 112140.
- (43) Fan, J.; Wang, S.; Zhang, X.; Chen, W.; Li, Y.; Yang, P.; Cao, Z.; Wang, Y.; Lu, W.; Ju, D. Quantum Dots Elicit Hepatotoxicity through Lysosome-Dependent Autophagy Activation and Reactive Oxygen Species Production. *ACS Biomater. Sci. Eng.* **2018**, *4*, 1418–1427.
- (44) Ching, H. S.; Luddin, N.; Rahman, I. A.; Ponnuraj, K. T. Expression of Odontogenic and Osteogenic Markers in DPSCs and SHED: A Review. *Curr. Stem Cell Res. Ther.* **2017**, *12*, 71–79.
- (45) Suzuki, S.; Haruyama, N.; Nishimura, F.; Kulkarni, A. B. Dentin sialophosphoprotein and dentin matrix protein-1: Two highly phosphorylated proteins in mineralized tissues. *Arch. Oral Biol.* **2012**, *57*, 1165–1175.
- (46) Liu, M. M.; Li, W. T.; Xia, X. M.; Wang, F.; MacDougall, M.; Chen, S. Dentine Sialophosphoprotein Signal in Dentineogenesis and Dentine Regeneration. *Eur. Cells Mater.* **2021**, *42*, 43–62.
- (47) Martin-Gonzalez, J.; Perez-Perez, A.; Cabanillas-Balsara, D.; Vilarino-Garcia, T.; Sanchez-Margalet, V.; Segura-Egea, J. J. Leptin stimulates DMP-1 and DSPP expression in human dental pulp via MAPK 1/3 and PI3K signaling pathways. *Arch. Oral Biol.* **2019**, *98*, 126–131.
- (48) Cui, D.; Xiao, J.; Zhou, Y.; Zhou, X.; Liu, Y.; Peng, Y.; Yu, Y.; Li, H.; Zhou, X.; Yuan, Q.; Wan, M.; Zheng, L. Epiregulin enhances odontoblastic differentiation of dental pulp stem cells via activating MAPK signalling pathway. *Cell Prolif.* **2019**, *52*, No. e12680.
- (49) Xie, Y.; Wan, B.; Yang, Y.; Cui, X.; Xin, Y.; Guo, L. H. Cytotoxicity and autophagy induction by graphene quantum dots with different functional groups. *J. Environ. Sci.* **2019**, *77*, 198–209.
- (50) Wang, B.; Yang, M.; Liu, L.; Yan, G.; Yan, H.; Feng, J.; Li, Z.; Li, D.; Sun, H.; Yang, B. Osteogenic potential of Zn(2+)-passivated carbon dots for bone regeneration in vivo. *Biomater. Sci.* **2019**, *7*, 5414–5423.
- (51) Li, X.; Liu, H.; Yu, Y.; Ma, L.; Liu, C.; Miao, L. Graphene Oxide Quantum Dots-Induced Mineralization via the Reactive Oxygen Species-Dependent Autophagy Pathway in Dental Pulp Stem Cells. *J. Biomed. Nanotechnol.* **2020**, *16*, 965–974.
- (52) Alers, S.; Löffler, A. S.; Wesselborg, S.; Stork, B. Role of AMPK-mTOR-Ulk1/2 in the regulation of autophagy: cross talk, shortcuts, and feedbacks. *Mol. Cell Biol.* **2012**, *32*, 2–11.
- (53) Kim, J.; Kundu, M.; Viollet, B.; Guan, K. L. AMPK and mTOR regulate autophagy through direct phosphorylation of Ulk1. *Nat. Cell Biol.* **2011**, *13*, 132–141.
- (54) Li, Y.; Chen, Y. AMPK and Autophagy. *Adv. Exp. Med. Biol.* **2019**, *1206*, 85–108.
- (55) Liu, X.; Chhipa, R. R.; Nakano, I.; Dasgupta, B. The AMPK inhibitor compound C is a potent AMPK-independent antiglioma agent. *Mol. Cancer Ther.* **2014**, *13*, 596–605.
- (56) Hulea, L.; Markovic, Z.; Topisirovic, I.; Simmet, T.; Trajkovic, V. Biomedical Potential of mTOR Modulation by Nanoparticles. *Trends Biotechnol.* **2016**, *34*, 349–353.